Image Cover Sheet

CLASSIFICATION	SYSTEM NUMBER
UNCLASSIFIED	105537

TITLE

APPLICATION OF RADON TRANSFORM TECHNIQUES TO WAKE DETECTION IN SEASAT-A SAR IMAGES

System Number:

Patron Number:

Requester:

Notes:

DSIS Use only:

Deliver to: JR

Application of Radon Transform Techniques to Wake Detection in Seasat-A SAR Images

Maria T. Rey
James K. Tunaley
J. T. Folinsbee
Paul A. Jahans
John A. Dixon
Malcolm R. Vant

Reprinted from
IEEE TRANSACTIONS ON GEOSCIENCE AND REMOTE SENSING
Vol. 28, No. 4, July 1990

Application of Radon Transform Techniques to Wake Detection in Seasat-A SAR Images

MARIA T. REY, JAMES K. TUNALEY, MEMBER, IEEE, J. T. FOLINSBEE, PAUL A. JAHANS, JOHN A. DIXON, MEMBER, IEEE, AND MALCOLM R. VANT, MEMBER, IEEE

Abstract—**A moving ship produces a set of waves in a characteristic linear "V" pattern. This pattern, or some of its components, can often be detected in ocean imagery produced by satellite-borne Synthetic Aperture Radar (SAR) sensors operating at *L*-band. Some wake components, notably the turbulent wake, may extend for 5–15 km behind the ship. As ship wake detection can provide information such as ship direction and speed, the detection of these wakes can play an important role in satellite surveillance of shipping. Described is research done on the use of the Radon transform to automatically detect ship wakes in Seasat ocean imagery. The objective of the research was twofold: to automatically detect ship wakes and to differentiate ship wakes from other linear ocean features produced by the underwater topography and existing sea conditions. An ADA (Automatic Detection Algorithm) based on the Radon transform was developed and applied to the Seasat imagery. The basic system performs the Radon transform of the SAR image, then detects bright and dark peaks produced in the transform by wakes (or other linear features) in the image. As the Radon transform essentially integrates the image intensity along every straight line through an image, each integral becomes one element in transform space. This integration process averages out the intensity fluctuations due to noise, thereby increasing the signal-to-noise ratio of the feature of interest in the transform space relative to that in the original image. A number of additional processing techniques were developed and tested to improve the PD (probability of detection) and reduce the PFA (probability of false alarm). To date, the use of an ADA, which combines a high-pass filter followed by a normalized Radon transform and a Wiener filter, has been shown to reliably distinguish wake peaks from false alarms.**

Keywords—**Wake, Radon, radar.**

I. Introduction

A MOVING ship produces a set of waves in a characteristic linear "V" pattern. This pattern, or some of its components, can often be detected in ocean imagery produced by satellite-borne SAR (Synthetic Aperture Radar) sensors operating at *L*-Band. For example, images produced using data from the Seasat-A SAR show ship wakes appearing as distinct straight lines on the ocean background, often extending for 5 to 15 km aft of the ship. Detection of these wakes can provide information about the ship, such as size, direction, and speed.

There are at least two reasons why it would be more advantageous to detect the wake rather than the ship itself: the wake feature is larger and more distinct than the ship, and the motion of the ship relative to the SAR platform causes the ship to appear displaced in azimuth from the wake, possibly into a high-clutter area, which can make it hard to detect. Therefore detection of the wake may be useful as a means of inferring the presence of a ship, even if the ship itself is difficult to detect.

This paper describes research done on the use of the Radon transform to automatically detect ship wakes in Seasat-A SAR ocean images. One of the principal challenges in automatically detecting wakes is distinguishing them from naturally produced linear features. Some examples of such features are internal waves generated by salinity or thermal gradients, features produced by the underwater topography, and wind waves. Fortunately, these naturally occurring ocean phenomena rarely remain linear for as long as a ship wake. To investigate the problem of distinguishing the longer of these natural linear features from ship wakes, we included both ship wakes and surrounding empty ocean scenes in our Seasat-A SAR imagery data set. The empty ocean images included examples of naturally occurring ocean phenomena.

A variety of detection algorithms based on the radon transform were developed and tested to improve the probability of detection of ship wakes and reduce the false alarm rate. To date, the use of a detection algorithm which combines a high-pass filter, Radon transform, and Wiener filter has been shown to reliably distinguish wake peaks from false alarms.

It should be noted that other authors have explored the area of ship-wake detection via the use of the Radon transform. Murphy [1] proves the viability of the technique for both simulated and real SAR images. Skingley and Rye [2] address post-processing problems, including the detection of peaks and troughs in the Hough domain and the removal of false alarms. Hendry [3] addresses the elevated false-alarm rate compared with the prediction of an analysis based on the central limit theorem and shows that the assumption of a normal distribution in the transform domain is not valid in the tails of the distribution.

Manuscript received October 20, 1989; revised March 5, 1990.

M. T. Rey and M. R. Vant are with Defence Research Establishment Ottawa, 3701 Carling Avenue, Ottawa, ON, Canada, K1A 0Z4.

J. K. Tunaley, P. A. Jahans, and J. A. Dixon are with London Research and Development, 755 Queens Avenue, London, ON, Canada, N5W 3H7.

J. T. Folinsbee is with Roy Ball Associates, 1750 Courtwood Crescent, Ottawa, ON, Canada, K2C 2B5.

IEEE Log Number 9036085.

A. The Radon Transform

The Radon transform of a continuous image is defined as

$$f(p, \theta) = \iint_D g(x, y)\, \delta(p - x \cos\theta - y \sin\theta) \tag{1}$$

where

D	entire image plane [4],
$g(x, y)$	grey level at position (x, y),
δ	Dirac delta function,
p	radius coordinate of a straight line,
θ	angle coordinate of a straight line.

The Radon transform accentuates straight-line features in an image by integrating image intensity along all possible lines in the image space. The integration over a line becomes a single point in the Radon transform space. If pixels along a line in an SAR image are, on average, of different intensity than the background, then a bright (higher than average) or dark (lower than average) peak should result in the transform space. Therefore a bright or dark spot in the transform domain corresponds to a bright or dark line in the image plane. It should also be noted that, because the integration process smooths out noise in the transform domain, the S/N (signal-to-noise ratio) is greater in the transform domain than in the image plane. Another valuable feature is that the Radon transform integration process does not depend on a line being continuous in nature, unlike other linear detection algorithms.

It is convenient to normalize the transform so as to produce a constant PFA (probability of false alarm) across the image field. Because the variance of the background noise is proportional to the integration line length in the Radon transform, the transformed image is adjusted by dividing each element by the square root of the length of the integration line associated with it. It should also be noted that constancy of the PFA does not result in a fixed probability of detection across the field: the probability of detection tends to be reduced, particularly for short features located near the edge of the image.

B. Research Objective

Since ship wakes are linear features, it was decided that the Radon transform would be the most appropriate algorithm for their detection. However, both wakes and naturally-occurring linear features will be detected by the application of the Radon transform. Therefore the objective of this work had to be twofold: first, to determine the utility of the Radon transform for detection of linear features in Seasat-A SAR wake imagery, and secondly, to assess the ability to distinguish wakes from other linear ocean features.

II. Seasat-A SAR Imagery

The images used in this study were extracted from digitally processed Seasat-A-SAR ocean imagery. These images include both ship-wake images and their surrounding ocean background scenes. It should be noted that in acquiring the data, land features were needed to determine the coordinates of ship wakes of interest. Hence the wake data used in this study consist mostly of wakes in coastal regions, where linear features induced by the underwater topography are abundant.

Ships appear in the images as small areas of extremely bright returns associated with one or more visible wake components. These wake components are generally discontinuous in nature, and are frequently displaced from the ship return. This occurs because SAR uses the Doppler shift of the returned target signal to determine the position of the target in azimuth. Hence the velocity of the ship can alter the recorded position of the ship. On the other hand, the returns from the ocean surface are not significantly Doppler-shifted, so that the image of the wake itself is not displaced. The exact offset depends on the speed and direction of the ship.

The wake images themselves also introduce variability into the problem. The wake can be divided into several components, some of which may or may not always be present. The principal components are the classical Kelvin wake, which is itself composed of the cusp waves, the divergent waves, and the transverse waves; the turbulent wake, which comprises the turbulent region directly behind the ship; and narrow-V wake components, which are probably associated with either the turbulent wake or reflections of ambient waves, both from the wake edges and the ship's hull. In coastal regions where conditions are right, there may also be ship-generated internal wave wakes. This variety in the wake components complicates the problem of automatic detection in that the actual wake pattern can vary greatly, depending on which components are present. Not all wake components are visible in all images, and this is probably because of their different orientations to the Seasat-A SAR sensor, in addition to variations in the ship size and speed, and varying ocean and wind conditions. The most frequently visible wake components were the dark turbulent wake and a form of the narrow-V wake associated with it [5].

III. Evaluation of the Radon Transform

A. Determination of Optimum Image Size

Performance of the Radon transform in the detection of linear features is maximized when the linear feature of interest is approximately the same size as the image dimensions. It was determined for our data that an image size of approximately 400 × 400 (6.4 km × 6.4 km) pixels gave optimum results. Given these results, a standard set of 26 400 × 400 pixel-wake images were used for the preliminary testing. Another set of 400 × 400 adjacent ocean images containing no visually obvious wake

components were also extracted to compare the Radon transforms of wake images to those of apparently uniform ocean regions.

B. Effect of Ship Returns on Transform Performance

Because the ships appear in the imagery as small areas of extremely bright returns, their effect on the transform is to "swamp" it with very bright sinusoids, making detection of wake peaks difficult. A threshold can be determined and used to detect the pixel values associated with the ship returns. Once detected, the area of the original image containing the ship returns can be replaced by the mean value of the image amplitude.

C. Radon Transform Performance

Prior to applying the Radon transform, the original images were prepared by subtracting the image mean from each pixel and applying a clipping process, which set all large values to a predetermined maximum value.

After application of the Radon transform, the original images were prepared by subtracting the image mean from each pixel and applying a clipping process, which set all large values to a predetermined maximum value.

After application of the Radon transform, an automatic detection algorithm (ADA) was applied to the data. The ADA first calculated the mean, m, and standard deviation, σ, of the Radon transform of the image. The performance of the ADA could then be assessed in terms of the ratio of the height of a peak (with mean subtracted), in the transform domain, to the standard deviation in the transform domain. This ratio is, for our purposes, defined to be the S/N ratio in the transform space. The detection threshold is set at $\pm K\sigma$. The choice of sign depends on whether bright or dark peaks are to be detected. K is a user-defined parameter, which was set equal to four for the initial trials. The Radon transform space is compared to this threshold, and a bitmap is produced of the bright or dark region of interest. The appearance of peaks above the positive threshold or below the negative threshold is indicative of the presence of a wake feature.

The transforms of the uniform ocean areas did not show very many features, although there was a characteristic pattern present. This pattern was associated with the sinusoidal curves produced, in part, by the transformation of the coherent speckle in the original image. The sinusoids are produced because a discrete point, such as produced by speckle noise in the original image, transforms into a sinusoid in the radon transform domain.

As expected, the transforms of the ship wake data contained peaks (or troughs) corresponding to each of the ship-wake arms. The ADA detected 21 out of 30 wake components (bright and dark wakes combined) for an overall PD (probability of detection) of 0.7. It detected 50% of the bright wake components and 25% of the dark wake components, visible by eye in the wake images. Visual examination of the transforms resulted in the detection of 29 out of 30 wake components. In general, the ADA did not detect the remaining peaks because they fell below the selected threshold, which had been set to 4σ.

Reduction of this threshold would improve the ADA performance for these peaks, but it would also increase the PFA substantially. It was found that the probability of detecting at least one ship-wake component in any image containing a wake was one over all the images. However, the FAR (false alarm rate) was typically twelve false alarms per 400 × 400 pixel image for bright wakes and four for dark wakes. Because the use of the Radon transform for wake detection is ultimately under consideration for satellite surveillance of shipping applications, where huge ocean areas must be covered at a time, the PFA values were judged to be unacceptably high. It was therefore concluded that improvements must be made to the ADA to increase the PD and reduce the PFA.

IV. Improvements to the Basic ADA

After taking the Radon transform of the preliminary data set, it was determined that features that are clearly visible to the eye produce obvious peaks or troughs in the transform domain. Unfortunately, in practice, true detections tend to be overwhelmed by false alarms. A number of different causes for this were considered. Among these were:

a) the effect of having speckle statistics that did not conform to the assumed model,
b) nonstationarity of the sea returns, which caused large-scale variations in the ocean radar cross section, and
c) poor matching of the transform to the image; this includes the selection of feature length with respect to the image size, and feature width relative to the Radon integration line.

To investigate the first two of these problems, the background sea was modeled as a two-dimensional field of 256 × 256 independent random variables, each with a Rayleigh distribution. Linear features of various intensities were then superimposed on this field and the Radon transform was taken. It was found that features that were just barely detectable by eye could be detected reliably in the Radon transform domain. Therefore it is clear that for ideal Rayleigh-distributed sea background, wake features are easily detected by the Radon transform, and hence it is, in part, the departure of the sea clutter statistics from this ideal that causes false alarms.

The effects of a mismatch between the integration length in the Radon transform and the feature length was investigated using both real and simulated images. The feature length size was reduced by varying amounts by means of nearest-neighbor averaging of adjacent pixels in the image plane, prior to calculation of the Radon transform. There proved to be little change in performance as the feature length was changed, so it was concluded that the mismatch of the integration lengths in the Radon domain to the length of the image feature was not the primary

performance problem. However, it did show that, provided only a few pixels were combined, performance was not degraded. Since the averaging technique reduced the number of pixels per image area as a side effect, it proved useful for increasing processing speed.

A. Sea-Surface Statistics

Sea-surface statistics exhibit a high degree of variance. When there are no strong linear features present, the image appears noise-like and virtually featureless. The only features that may be visible are the long gravity sea waves, which can be seen as light and dark banding on the noise amplitude, and possibly internal waves. This was confirmed by examination of Seasat images. It was also noted that, despite their fairly coarse resolution (25 m), the statistical distributions of the Seasat images were often not Rayleigh. Deviations from Rayleigh statistics can be caused by sea spikes on the ocean surface in combination with coherent speckle from the SAR. The statistics can be described by the K distribution, as discussed by Ward and Watts [6].

The Radon transform of an impulse, or spike, is a sinusoid. Thus the high-amplitude pixels, which contribute to the tail of the amplitude distribution, will cause a large number of large sinusoidal features in the transform domain. These sinusoids tend to obscure the presence of the more point-like features in the transform space, which are associated with actual ship wakes.

B. Spectral Characteristics of Sea Images

The two-dimensional spectral density of the pixel amplitudes for a number of sea scenes has been calculated. When the pixel amplitude distribution is compared to the Rayleigh distribution and a value of chi-squared per degree of freedom of the order of one is exhibited, the spectral density is typically featureless. It just falls slowly to small values as spatial frequencies, corresponding to the reciprocal of the resolution cell size, are approached. However, for cases in which the value of chi-squared per degree of freedom is greater than ten, the spectral density often exhibits strong low-frequency components.

The low-frequency features in the spectral density of sea scenes represent slow variations across the image plane and are often not obvious to the eye. The effect of these variations on the Radon transform is to produce fluctuations in the local mean over large image areas. When these areas are integrated along a Radon integration line, the variations in the mean often cause large shifts in the background level in the Radon domain. This can produce a serious problem with false alarms.

These characteristics suggest that a simple filter, which removes the effects of the low-frequency components, should be applied to the image before the transform is performed.

C. The Running Mean Filter

Fig. 1 shows the image of a wake in which the wake components in the image are detectable by eye (though not very clearly). Fig. 2 shows the Radon transform of the same image. The ratio of the maximum to the standard deviation in the transform domain is 8.6. Although it is possible to distinguish in the transform all the wake components visible by eye, the associated number of ADA false alarms is high. It was therefore decided to investigate the use of techniques which increased the S/N in the image, in an attempt to lower the number of false alarms.

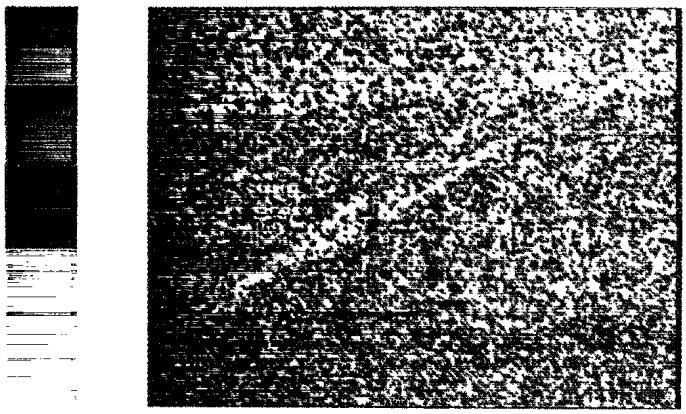

Fig. 1. Seasat image of ship wake.

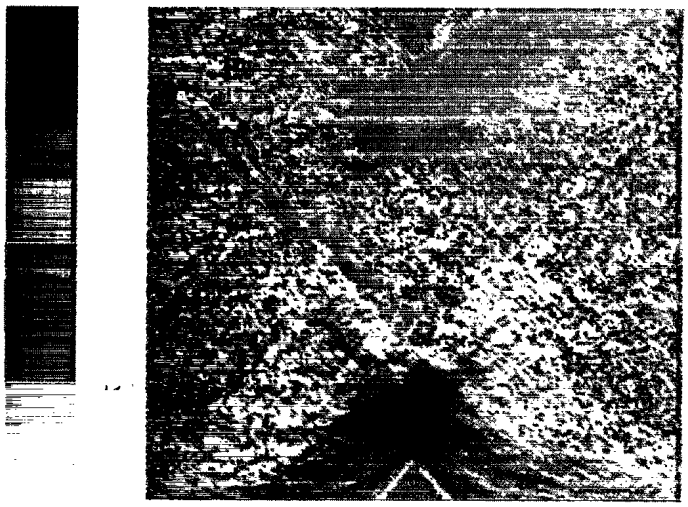

Fig. 2. Radon transform of Fig. 1.

Prior to this experiment, the image was first contracted by a factor of three in each direction to reduce the processing time. This was done by adding the amplitudes of adjacent pixels in groups of 3×3 pixels. This process is separate and distinct from the running mean filter application.

To increase the S/N ratio, a running mean filter was applied to the image data. This filtering operation consisted of subtracting a local mean value from each pixel amplitude. The local mean was found from the data within a square window centered on the pixel. Varying window sizes, ranging from 2×2 to 40×40 pixels, were used. A comparison of the Radon transforms showed that, in general, the effect of the filtering was to make the background essentially featureless, leaving pure speckle noise.

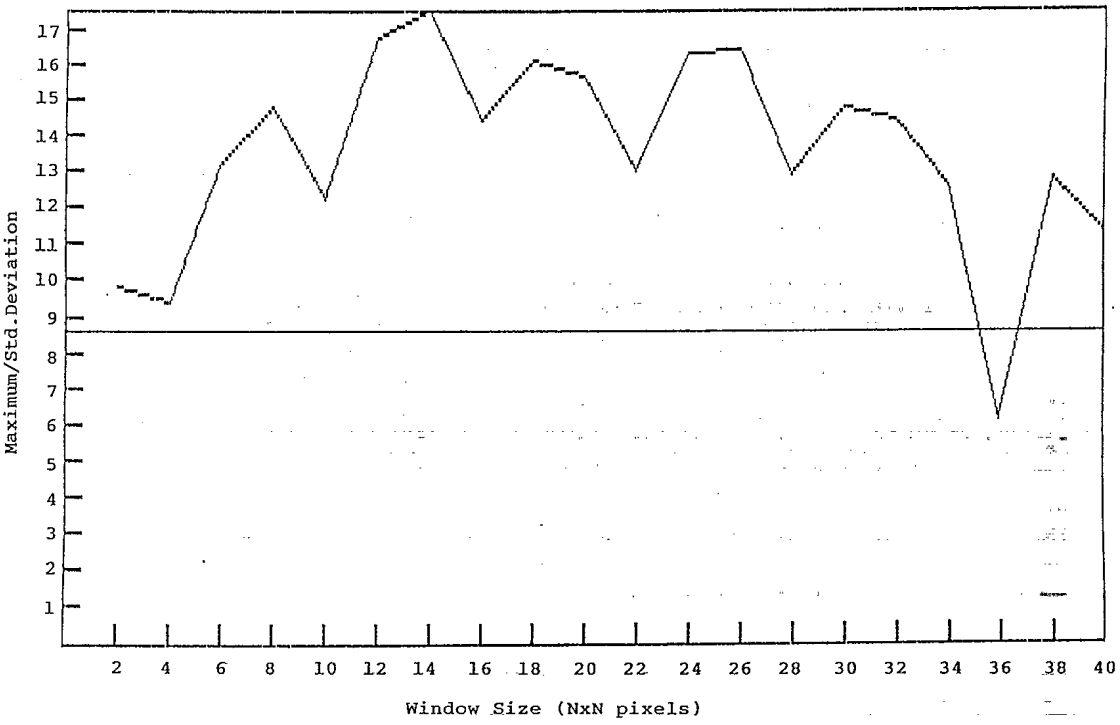

Fig. 3. Plot of S/N ratio versus window size for radon transform of ship wake image.

As expected, when the window size approached the size of the image, the effect of the filtering disappeared. Fig. 3 shows a plot of the S/N ratio versus window size for the Radon transform of a wake image. The S/N ratio for this image increases from 8.6, without filtering, to 17.5, with filtering—an increase of 103% (in fact, at a window size of 15 × 15, the S/N ratio reached 19.1, or 122%). The horizontal line running through the plot shows the S/N level of the radon transform for the unfiltered image.

The 15 × 15 running mean high-pass filter was chosen for application to several wake images. Each of these images was first contracted by two to increase the processing speed. The filtering produced a significant increase in S/N in all cases, and hence increased the detectability of the wake components. Both dark and bright wake detectability was enhanced using this technique.

The improvement in the S/N ratio is important because the PFA falls off very rapidly with increasing S/N ratio. A 10% increase in the S/N ratio for an image implies an order of magnitude reduction in the PFA. It is possible that further gains could result from the application of more sophisticated filters.

D. The Wiener Filter

Mismatch between the shape of the peak caused by the linear wake feature in the Radon transform domain and the integration length in the Radon transform can be compensated for by the application of a filter after the transform has been performed. In this case the filter becomes a peak-shape detector. The Wiener filter is used to match the shape and magnitude of a candidate wake peak to some predetermined ideal peak. The ideal peak must be representative of the typical Radon peak shape and its size relative to the noise background. Since the size is indeterminate before the measurement, the height of the filter is set to a value such that the filter performs optimally in a band of amplitudes centered about the threshold of detection. Peaks whose amplitudes fall above this band will be detected, and smaller peaks that have amplitudes lying below this band will not be detected. Peaks whose amplitudes lie within the band are tested with the Wiener filter to determine whether or not they should be detected.

The Wiener filter is an optimum nonrecursive linear estimator giving solutions to the Wiener–Hopf equation. The Wiener filter takes the signal and noise vector and tries to estimate the signal in the least squares sense. The derivation is given by Bozic [7], and is easily understood for the case of a one-dimensional signal. In scalar form, a single estimate of a signal value in noise is given by

$$\hat{x} = \sum_{i=1}^{m} h(i)\, y(i) \tag{2}$$

where $y(1)$, $y(2)$, $\cdots$, $y(m)$ are data signals and $h(1)$, $h(2)$, $\cdots$, $h(m)$ are filter weights corresponding to the data signals. The objective is to choose the filter coefficients such that the mean-square error

$$P_e = E\left((x - \hat{x})^2\right) \tag{3}$$

is minimized.

For the case of the vector Wiener filter, applicable to the present problem, the assumed signal is in the form of an input array, which is a collection of pixel amplitudes that correspond to a Radon peak and its immediate neighborhood, minus the noise.

The size to use for this array is determined by the extent of a typical Radon peak. Here the size was chosen to be 7×7 pixels. The goal of the Wiener filter is to provide an estimate of this assumed signal in the presence of noise.

Unfortunately, the signal is spatially variant. The implication of this is that the data samples vary not only because of the additive noise, but also because of signal variations within the sample window. Thus the filter coefficients must be represented by a 7×7 matrix corresponding to the two-dimensional window.

E. The Wiener Filter in the Radon Domain

The output signal required from the transform system is a set of numbers representing the maxima (or minima) for a 7×7 window around the strong peaks in the Radon domain. For simplicity, it was assumed that a single peak could be approximated by a Gaussian shape, where the height of the peak relative to the root mean square noise level in the Radon domain was taken to be five times the standard deviation of the noise. This was intended to produce a filter optimized for signals on the threshold of detectability.

In modeling the shape of the peak as a Gaussian function, the distance of a point from the center of the filter window was taken to be r pixels. The noise was assumed to be white with a mean of zero and unit variance, and to be uncorrelated with the signal. Thus the data points, y, were assumed to be of the form

$$y = 5 \exp\left(-r^2/2d^2\right) + n \qquad (4)$$

where d is a measure of the peak width in the Radon domain (chosen empirically to match the typical Radon peak widths), and n is the noise.

The Wiener filter program implements two filters: one for bright peaks and another for dark peaks.

Before the application of the Wiener filter, the two-dimensional automatic detection algorithm is first applied with a threshold set at ± 4.5 times the standard deviation of the noise. The ADA returns a list of peaks in the Radon domain which pass this threshold. The Wiener filter is then applied to these peaks.

F. Filter Tests on Real Data

Two tests of the overall transform system were tried on a set of 17 ship wake images. These are shown in Tables I and II as Runs #1 and #2. Each of these tests was conducted with a different set of widths in the Wiener filter. These widths were specified in terms of the variable d in the Gaussian model. Each set of widths is subdivided into a subset for bright peaks and a subset for dark peaks. The dark peak subset uses slightly larger widths. In Run #1, the Gaussian function was 2.5 pixels wide for bright peaks and 3.75 pixels for dark peaks. In Run #2, widths of 6.25 and 7.5 pixels were used for bright and dark peaks, respectively. These widths are the values of d described in (4). The figures apply to the original image.

The images used in the testing were chosen because their transforms exhibited low S/N ratios. No image was used, which when unfiltered contained a peak in the transform domain of amplitude greater than seven standard deviations. It should be noted that all images were preprocessed and then contracted in size, by averaging, to remove returns from the ship and speed up the processing. A high-pass filter (running mean filter) was then used to remove broad features in the sea background. Next, a normalized Radon transform was applied, followed by a Wiener filter.

The estimates of the width of the Gaussian function were confirmed by applying the Wiener filter to the Radon transforms of some images. The performance versus es-

TABLE I
RUN #1 SUMMARY

Image	Wake Value	Wake/SD	FA Value	Wake Gain	FA Gain	Gain Ratio
1.	−0.0135	−3.2	−0.0136	0.926	0.833	1.113
2.	0.0073	5.5	0.0058	1.283	1.174	1.093
3.	−0.0075	−4.1	−0.0090	1.158	0.308	3.760
4.	NA	NA	0.0180	NA	0.867	NA
4.	NA	NA	−0.0175	NA	0.628	NA
5.	−0.0174	−4.3	NA	0.924	NA	NA
5.	NA	NA	0.0174	1.062	NA	NA
6.	0.0143	5.6	0.0108	1.180	1.070	1.103
7.	NA	NA	0.0039	NA	0.451	NA
7.	NA	NA	−0.0039	NA	0.283	NA
8.	NA	NA	−0.0082	NA	0.260	NA
9.	−0.0106	−5.4	−0.0109	0.713	0.539	1.322
10.	−0.0112	−4.7	−0.0080	0.643	0.360	1.789
11.	0.0297	8.2	0.0165	0.882	0.854	1.033
11.	−0.0178	−4.9	−0.0115	0.818	0.635	1.288

Note: Wake value = maximum absolute height of peak in radon domain. FA value = height of greatest false alarm in radon domain.

TABLE II
RUN #2 SUMMARY

Image	Wake Value	Wake/SD	FA Value	Wake Gain	FA Gain	Gain Ratio
12.	0.0141	5.0	0.0148	0.841	0.547	1.538
12.	NA	NA	−0.0119	NA	0.327	NA
13.	−0.0123	−4.3	−0.0121	0.400	0.224	1.787
13.	NA	NA	0.0131	NA	0.305	NA
1.	−0.0150	−3.6	−0.0136	0.464	0.351	1.321
14.	0.0227	6.8	NA	0.669	NA	NA
14.	−0.0196	−5.9	−0.0138	0.373	0.190	1.959
2.	0.0073	5.5	0.0067	0.591	0.459	1.287
3.	−0.0075	−4.1	−0.0090	0.720	0.157	4.586
4.	NA	NA	0.0180	NA	0.197	NA
4.	NA	NA	−0.0175	NA	0.187	NA
5.	−0.0174	−4.3	NA	0.433	NA	NA
5.	NA	NA	0.0174	0.428	NA	NA
6.	0.0143	5.6	0.0108	0.555	0.335	1.656
15.	NA	NA	0.0091	NA	0.330	NA
15.	NA	NA	−0.0091	NA	0.1.75	NA
16.	NA	NA	0.0088	NA	0.534	NA
17.	NA	NA	−0.0067	NA	0.303	NA
7.	NA	NA	0.0039	NA	0.254	NA
7.	NA	NA	−0.0039	NA	0.225	NA
9.	−0.0106	−5.4	−0.0109	0.410	0.288	1.422
10.	−0.0112	−4.7	−0.0079	0.358	0.193	1.854
11.	0.0297	8.2	0.0179	0.270	0.259	1.040
11.	−0.0178	−4.9	−0.0114	0.431	0.228	1.890

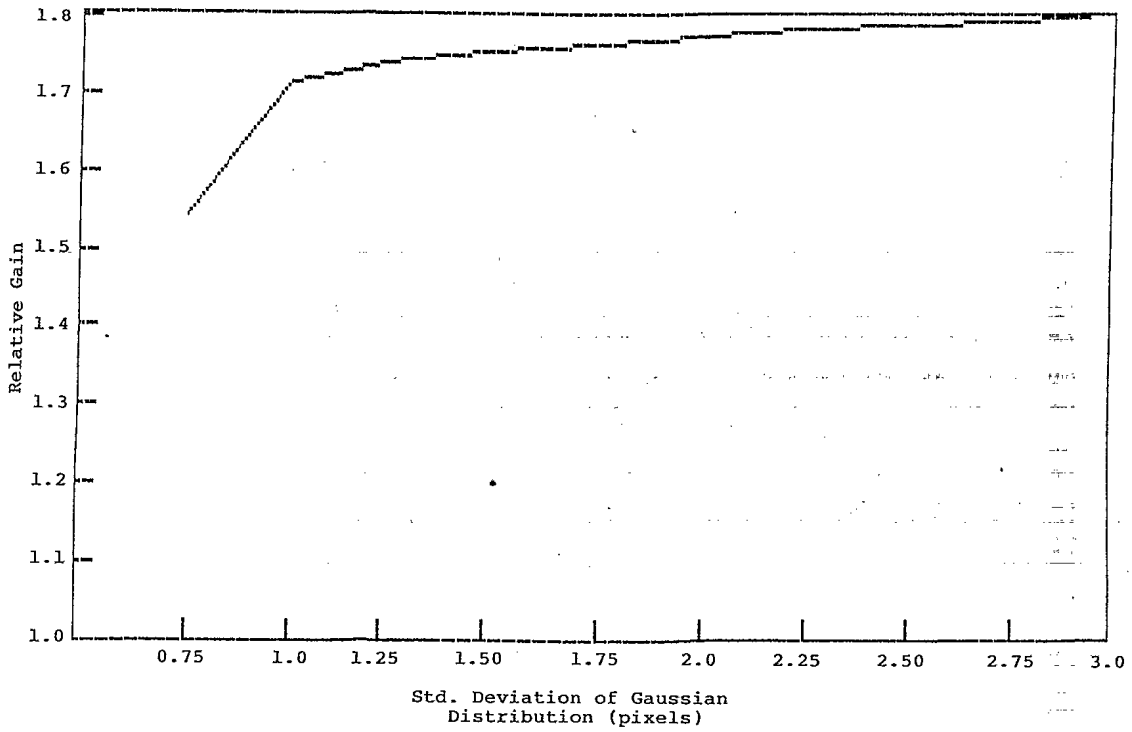

Fig. 4. Plot of Wiener filter gain ratio versus estimated peak width for sample transform image.

timated width was measured in terms of the ratio of the Wiener filter gain for a wake peak to that for a false alarm. Here the Wiener filter gain is defined as the ratio of the size of the peak after filtering to that before filtering. The gain ratio was considered to be the best measure of the Wiener filter's ability to separate wake peaks from false alarm peaks. Fig. 4 shows a plot of the Wiener filter gain ratio versus the estimated peak width for an example transform image. It was found from these plots that the performance of the filter was insensitive to the width of the Gaussian function that was chosen.

Tables I and II form a complete summary of the results of Runs #1 and #2. The gain ratio describes the separation between wakes and false alarms achieved through the use of the Wiener filter. The false alarm intensity chosen for comparison purposes was the one which produced the highest Wiener filter gain. The main result to be noted from these tables is that, as expected, the gain ratio is most often highest for those Radon peaks that are close to 5 in height.

A possible detection scheme using the Wiener filter would employ the following rule base. Any peaks in the radon domain which are greater than 6 would almost certainly represent valid linear features, even in a large image. Similarly, any Radon peak of a value less than 4.5 would not be classified as a linear feature. In between these thresholds, the Wiener filter would be used to make a decision. Any peak producing a Wiener filter gain greater than some predetermined threshold would be considered a detection. Anything below that threshold would be considered a false alarm. For example, when using a Gaussian function width that is reasonably close to optimal for the data of runs #1 and #2, the thresholds on the Wiener filter gain for bright and dark wakes were set to 0.55 and 0.4, respectively.

V. Conclusion

The Radon transform combined with a simple Automatic Detection Algorithm can detect almost all visible wakes in an image. However, the PFA associated with the use of these techniques alone is unacceptably high for satellite ship surveillance applications.

The most promising technique for reducing the PFA that we have discovered to date centers around using a simple Radon transform for the actual wake detection, augmented with preprocessing and postprocessing to reduce the number of false alarms.

The preprocessing involves high-pass filtering of the data to remove background sea effects. This preprocessing step alone is capable of doubling the S/N ratio. This implies that significant low-frequency sea structure is present but is not necessarily visible to the eye, and that this sea structure is at least partially responsible for the high PFA obtained when the data are not high-pass filtered.

The postprocessing involves the application of a peak-shape detector based on the Wiener filter. Using this technique, the gain from the use of the shape detector is used for discrimination between wake peaks and false alarms.

For the 39 wakes analyzed in this study, the results were extremely promising. All wakes visible by eye were detected (at least one wake component per wake) and there was one false alarm. A selection of sea scenes was also analyzed. No wakes were detected for the sea scenes, and

there were no false alarms. The Wiener-filter gain-detection thresholds used to classify the peaks were 0.55 and 0.4 for bright and dark wake peaks, respectively.

REFERENCES

[1] L. M. Murphy, "Linear feature detection and enhancement in noisy images via the Radon transform," *Pattern Recognit. Lett.*, vol. 4, no. 4, pp. 279–284, Sept. 1986.

[2] J. Skingley and A. J. Rye, "The Hough transform applied to SAR images for thin line detection," *Pattern Recognit. Lett.*, vol. 6, no. 1, pp. 61–67, June 1987.

[3] A. Hendry, J. Skingley, and A. J. Rye, "Automated linear feature detection and its application to curve location in Synthetic Aperture Radar imagery," in *Proc. IGARSS'88 Symp.* (Edinburgh, UK), Sept. 1988, vol. 2, pp. 1521–1524.

[4] S. R. Deans, "Hough transform from the Radon transform," *IEEE Trans. Pattern Anal. Mach. Intell.*, vol. 3, no. 2, pp. 185–188, Mar. 1981.

[5] J. K. Tunaley, E. H. Buller, K. H. Wu, and M. T. Rey, "The simulation of the SAR image of a ship wake," *IEEE Trans. Geosci. Remote Sensing*, vol. 28, Nov. 1990, to be published.

[6] K. D. Ward and S. Watts, "Radar sea clutter," *Microwave J.*, vol. 28, no. 6, pp. 109–121, June 1985.

[7] S. M. Bozic, *Digital and Kalman Filtering*. London: Edward Arnold, 1979.

*

Maria T. Rey received the B.Sc. degree in engineering physics at Dalhousie University, Halifax, Nova Scotia, and the M.A.Sc. degree in electrical engineering at the Technical University of Nova Scotia in 1987.

She has been working since 1983 in the Airborne Radar Group, Radar Division, of the Defense Research Establishment Ottawa in Ottawa, ON. Her work has primarily involved synthetic aperture radar (SAR) remote-sensing applications, notably ship wake detection from space-based SAR's, SAR ship-wake modeling and ship classification, as well as airborne SAR polarimetric detection of man-made targets.

*

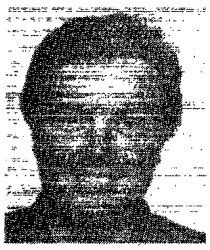

James K. Tunaley (M'82) received the B.Sc. and Ph.D. degrees from the University of Sheffield in 1962 and 1967, respectively. His postgraduate work was in the field of space physics.

From 1967 to 1970 he was at the European Space Technology Centre acting as Project Scientist for a number of sounding rocket payloads and a satellite payload. In 1971 he moved to the Physics Department of the University of Western Ontario and worked on probability theory and random walks. He founded London Research and Development in 1980. His current interests include radar image simulation and classification, the effect of the ionosphere in transionospheric communications, and the hydrodynamics of ship motions and ship wakes.

Dr. Tunaley is a Past Chairman of the London section of the IEEE.

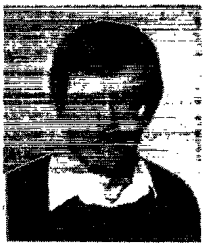

J. T. Folinsbee received the B.Sc. degree from the University of Alberta in 1969, and the M.S. and Ph.D. degrees in physics from the University of Illinois in 1971 and 1974.

He taught and did research in solid-state physics at Queen's University in Kingston and at Dalhousie University in Halifax until 1984. He then joined IMAGO, where his current interests include signal processing, image analysis, and pattern recognition.

*

Paul A. Jahans was born in 1964 at London, ON. He graduated from Fanshawe College as an Electrical Engineering Technologist in 1988.

That year, he joined London Research and Development. He has constructed phase-locked receivers for the reception of satellite signals and has implemented neural networks in hardware. His interests are in the application of methods of artificial intelligence to problems of signal processing and radar image classification.

*

John A. Dixon (M'88) was born in London, ON, in 1962. He graduated as an engineer from the University of Western Ontario in 1988 with a concentration in computer science. Since then, he has been at London Research and Development. Among his interests are microprocessor control, the processing of radar images, and the classification of images of ship wakes. He is also working on the application of neural network hardware.

Mr. Dixon is a Secretary of the Executive Committee of the London section of the IEEE.

*

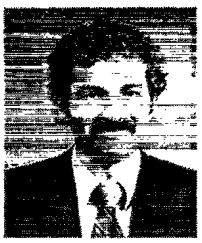

Malcolm R. Vant (S'73–M'75) received the Ph.D. degree in electrical engineering from Carleton University in Ottawa, Canada, in 1976.

From 1974 to 1976 he worked for Environment Canada on techniques for the microwave remote sensing and measurement of the dielectric properties of ice. In 1976 he joined the Airborne Radar Program at the Communications Research Centre, Communications Canada, in Ottawa. He has developed several software-based signal processors for synthetic aperture radar and methods of automatically focusing SAR images. During the period 1984–1986 he acted as the Scientific Authority for the ground-based processor for the Canadian RADARSAT Section at the Defence Research Establishment of Ottawa, where he directs research on all aspects of airborne radar.

NO. OF COPIES NOMBRE DE COPIES	COPY NO. COPIE N°	INFORMATION SCIENTIST'S INITIALS INITIALES DE L'AGENT D'INFORMATION SCIENTIFIQUE
1	1	AUG 12 1992 DAG

AQUISITION ROUTE FOURNI PAR ▶	DREO
DATE ▶	17 January
DSIS ACCESSION NO. NUMÉRO DSIS ▶	92-02694

DND 1158 (6-87)

National Defence / Défense nationale

9 #105537

PLEASE RETURN THIS DOCUMENT TO THE FOLLOWING ADDRESS:

DIRECTOR
SCIENTIFIC INFORMATION SERVICES
NATIONAL DEFENCE
HEADQUARTERS
OTTAWA, ONT. - CANADA K1A 0K2

PRIÈRE DE RETOURNER CE DOCUMENT À L'ADRESSE SUIVANTE:

DIRECTEUR
SERVICES D'INFORMATION SCIENTIFIQUES
QUARTIER GÉNÉRAL
DE LA DÉFENSE NATIONALE
OTTAWA, ONT. - CANADA K1A 0K2

CRAD / DRDIM 3
DEPARTMENT OF NATIONAL DEFENCE
OTTAWA ON K1A 0K2
CANADA